International Journal of Biological Macromolecules 85 (2016) 451–459

Contents lists available at ScienceDirect

International Journal of Biological Macromolecules

journal homepage: www.elsevier.com/locate/ijbiomac

Engineering of a novel tri-functional enzyme with MnSOD, catalase and cell-permeable activities

Piriya Luangwattananun[a], Sakda Yainoy[a,b,*], Warawan Eiamphungporn[a,b], Napat Songtawee[c,d], Leif Bülow[e], Chartchalerm Isarankura Na Ayudhya[b], Virapong Prachayasittikul[b,*]

[a] Center for Research and Innovation, Faculty of Medical Technology, Mahidol University, Bangkok 10700, Thailand
[b] Department of Clinical Microbiology and Applied Technology, Faculty of Medical Technology, Mahidol University, Bangkok 10700, Thailand
[c] Department of Community Medical Technology, Faculty of Medical Technology, Mahidol University, Bangkok 10700, Thailand
[d] Department of Clinical Chemistry, Faculty of Medical Technology, Mahidol University, Bangkok 10700, Thailand
[e] Pure and Applied Biochemistry, Department of Chemistry, Lund University, SE-221 00 Lund, Sweden

ARTICLE INFO

Article history:
Received 19 November 2015
Received in revised form 5 January 2016
Accepted 5 January 2016
Available online 8 January 2016

Keywords:
MnSOD
Catalase
Fusion protein
Oxidative stress
HIV-1 TAT
Protein engineering

ABSTRACT

Cooperative function of superoxide dismutase (SOD) and catalase (CAT), in protection against oxidative stress, is known to be more effective than the action of either single enzyme. Chemical conjugation of the two enzymes resulted in molecules with higher antioxidant activity and therapeutic efficacy. However, chemical methods holds several drawbacks; e.g., loss of enzymatic activity, low homogeneity, time-consuming, and the need of chemical residues removal. Yet, the conjugated enzymes have never been proven to internalize into target cells. In this study, by employing genetic and protein engineering technologies, we reported designing and production of a bi-functional protein with SOD and CAT activities for the first time. To enable cellular internalization, cell penetrating peptide from HIV-1 Tat (TAT) was incorporated. Co-expression of CAT-MnSOD and MnSOD-TAT fusion genes allowed simultaneous self-assembly of the protein sequences into a large protein complex, which is expected to contained one tetrameric structure of CAT, four tetrameric structures of MnSOD and twelve units of TAT. The protein showed cellular internalization and superior protection against paraquat-induced cell death as compared to either complex bi-functional protein without TAT or to native enzymes fused with TAT. This study not only provided an alternative strategy to produce multifunctional protein complex, but also gained an insight into the development of therapeutic agent against oxidative stress-related conditions.

1. Introduction

Oxidative stress has been known to associate with onset and/or progression of many diseases. To handle such condition, three major antioxidant enzymes including superoxide dismutase (SOD), catalase (CAT) and glutathione peroxidase (GPx) have been evolved. SOD is a primary antioxidant enzyme that catalyzes the dismutation of superoxide radical ($O_2^{\bullet -}$) into hydrogen peroxide (H_2O_2). In human, three isoforms of SOD have been characterized; CuZnSOD or SOD1, MnSOD or SOD2 and ECSOD or SOD3. Among the three, MnSOD or SOD2 which localizes in the mitochondrial compartment is believed to be the most important one since mitochondria is considered as the main ROS production site [1]. MnSOD is not only essential for the survival of all aerobic organisms [2] but has also been shown to be a powerful protective and therapeutic agent against oxidative stress-related conditions such as renal impairment [3], arthritis [4], chronic inflammation and lung fibrosis [4]. Another important antioxidant enzyme is CAT which functions to detoxify H_2O_2 into water (H_2O) and oxygen (O_2). Therapeutic uses of CAT were evidenced in various studies such as prevention and alleviation of neurological diseases [5] and pulmonary vascular oxidative stress [6]. To maximize protective and therapeutic efficiency, combinatorial use of SOD and CAT has been recommended. Chemical linkage of the two enzymes have provided better antioxidant activity and improved therapeutic efficacy [7,8]. However, chemical approach holds several drawbacks such as time-consuming, the need of chemical residues removal, loss of enzymatic activities during the process and non-homogeneity of the products. Conjugation of the two enzymes using gene fusion

* Corresponding authors. Tel.: +66 2 4414371-5; fax: +66 2 4414380.
E-mail addresses: sakda.yai@mahidol.ac.th (S. Yainoy), virapong.pra@mahidol.ac.th (V. Prachayasittikul).

http://dx.doi.org/10.1016/j.ijbiomac.2016.01.021
0141-8130/

technology has been proposed since 1989 [7]. Nevertheless, no successful production by this mean has been reported. Beside antioxidant activity, cell-permeable property is also critical for intracellular application of therapeutic proteins. To incorporate or enhance this property, cell penetrating peptide (CPP) can be applied. One of the most effective CPPs is HIV-1 TAT protein transduction domain (TAT), amino acid 49–57 (YGRKKRRQRRR). The peptide has been shown to transcellularly transport various protein cargos into living mammalian cells without disturbing original function of the proteins [9,10]. Unlike other CPPs, size of the cargos did not seem to affect transduction ability of this peptide [11]. Moreover, the non-cell type specificity of TAT transduction broadens the application with various cell types and disease models.

In this study, we described a strategy using protein engineering and recombinant DNA technology to produce a novel tri-functional protein with MnSOD, CAT and cell-permeable activities. cDNA encoding human CAT and MnSOD were fused in-frame and cloned into multiple cloning sites (MCS)-2 of pETDuet-1 plasmid. Then the fusion gene was co-expressed in *Escherichia coli* BL21 (DE3) with chimeric 6His-MnSOD-TAT gene, cloned in MCS-1 of the same plasmid. The two fusion proteins were proven to assemble into a large protein complex. Antioxidant activities, cell-permeable activity and protection against oxidative stress-induced cell death were investigated.

2. Materials and methods

2.1. Bacterial strains, plasmids and cell line

All bacterial strains and plasmids (pET46 and pETDuet-1) were obtained from Novagen (Novagen, EMD Bioscience, Germany). *E. coli* strain Novablue and BL21(DE3) were used as cloning and expression hosts, respectively. Mouse fibroblast (L929) cell line was ordered from American Type Tissue Culture Collection (ATCC, VA, USA).

2.2. Chemicals

Hydrogen peroxide 30% was from Merck, Germany and was standardized using the extinction coefficient of $43.6\,M^{-1}cm^{-1}$ at 240 nm [12]. δ-Aminovulinic acid, nitrotetrazolium blue chloride (NBT), NADH, phenazine methosulfate (PMS), paraquat (98% methyl viologen dichloride hydrate), bovine erythrocyte CuZnSOD and bovine liver catalase were obtained from Sigma–Aldrich (MO, USA). MTS reagent (Cell Titer 96® Aqueous One Solution) was from Promega Corporation (WI, USA). Alexa Flour® 488 protein labeling kit and fetal bovine serum (FBS) were ordered from Invitrogen (OR, USA). Hyclone® DMEM/High glucose was ordered from Hyclone Laboratories Inc. (UT, USA).

2.3. DNA manipulation for expression of chimeric proteins

Construction of plasmid expressing human MnSOD (pET46-MnSOD), human CAT (pET46-CAT), chimeric MnSOD-TAT (pET46-MnSOD-TAT) and chimeric CAT-TAT (pET46-CAT-TAT) were previously described [13–15]. To construct MnSOD-CAT (MC) fusion gene, DNA manipulation using In-Fusion cloning technology was performed. The cloning procedure was done according to manufacturer's protocol (Clontech Laboratories Inc., Japan). The primers used for PCR amplification of the two genes were designed to contain complementary regions with pETDuet-1 plasmid (shown as underlined text in Table 1). The reverse primer for MnSOD gene and the forward primer for catalase gene were designed to contain complementary sequences (shown as bolded text). After pETDuet-1 was treated with *Nde*I and *Xho*I, the vector and the two PCR products were combined and treated with In-Fusion enzyme. Then the In-Fusion mixture was transformed into *E. coli* Novablue strain. The resulting plasmid was designated as pETDuet-MC. Construction of CAT-MnSOD (CM) fusion gene was also done in the same manner as MC fusion gene. The used primers are listed in Table 1. The resulting plasmid was named as pETDuet-CM. To enable expression of the CM fusion protein, the chimeric gene was designed to co-express with native MnSOD gene. *Xho*I restriction site in pET46-MnSOD was replaced with *Not*I by site-directed mutagenesis (Agilent Technology, USA). Then the native gene was excised by treating with *Xba*I and *Not*I and inserted into MCS-1 of pETDuet-1, carrying CM fusion gene in MCS-2, pretreated with the same restriction enzymes. The resulting plasmid was designated as pETDuet-MnSOD/CAT-MnSOD (pETDuet-M/CM) (Fig. 1). To facilitate mammalian cell transduction of the CM fusion protein, the chimeric CM gene was co-expressed with chimeric MnSOD- TAT gene. Gene encoding chimeric MnSOD-TAT gene was removed from pET46-MnSOD-TAT and inserted into MCS-1 of pETDuet-1 carrying CM fusion gene in MCS-2. The resulting plasmid was designated as pETDuet-MnSOD-TAT/CAT-MnSOD (pETDuet-M-TAT/CM). All constructed plasmids were subjected to DNA sequence analysis to verify the accuracy of cloning procedure.

2.4. Protein expression and purification by IMAC

6His-MnSOD, 6His-CAT, 6His-MnSOD-TAT and 6His-CAT-TAT were expressed and purified as previously described [14–16]. The pETDuet-MC, pETDuet-CM, pETDuet-M/CM and pETDuet-M-TAT/CM plasmids were transformed into *E. coli* BL21(DE3). Cells were grown in 6 l of modified terrific broth supplemented with 100 μg ml^{-1} ampicillin at 37 °C, 180 rpm for 10 h. To induce protein expression, cultures were supplied with 1 mM IPTG. To facilitate MnSOD folding, 50 ppm of $MnCl_2$ was included in the culture medium and 0.3 mM δ-aminovulinic acid was supplemented to improve catalase heme content. The cultivation was continued for 16 h at 30 °C with shaking at 120 rpm. Cells were harvested, washed and resuspended in sonication buffer, 50 mM Tris–HCl, pH 7.8 containing 500 mM NaCl. Then cells were disrupted by sonication. The supernatant and pellet were separated by centrifugation at 14,000 rpm for 10 min at 4 °C. Prior to purification, crude extracts were filter-sterilized. For protein purification, the crude extracts were loaded onto Ni-NTA agarose IMAC column pre-equilibrated with sonication buffer attached to ÄKTA prime protein purification system (GE healthcare life sciences, UK) and eluted with gradient imidazole up to 0.5 M in the same buffer. Fractions were subjected to SDS-PAGE analysis then highly purified fractions were pooled and concentrated by 100 K Amicon® Ultra-15 centrifugal filter devices (EMD Millipore Corporation, MA, USA).

2.5. Protein purification and molecular weight determination by gel filtration chromatography

Gel filtration chromatography was used for protein purification and molecular weight (MW) determination. To separate mixture between tetrameric 6His-MnSOD or 6His-MnSOD-TAT and chimeric protein complex (Fig. 1) from the co-expression condition, IMAC-purified proteins were loaded onto Sephacryl S-300HR gel filtration chromatography column equilibrated with 50 mM sodium phosphate buffer, pH 7.8 containing 150 mM NaCl. The proteins were eluted with the same buffer. Standard proteins with known MW, ranging from 13.7 to 440 kDa, were used for standard curve preparation. All experiments were run by ÄKTA prime protein purification system and analyzed by PrimeView software. In addition, the MW of the proteins was further studied by static light scattering according to manufacturer's protocol (Malvern Instruments, UK).

Table 1
Primers for construction of chimeric MnSOD-CAT and CAT-MnSOD gene.

Primers	DNA sequences (5′ → 3′)
MnSOD FP[a] for construction of MC[b]	GAGATATACATATGAAGCACAGCCTC
MnSOD RP[c] for construction of MC	**CCGGCTGTCAGCCAT**CTTTTTGCAAGCCAT
CAT FP for construction of MC	**ATGGCTGACAGCCGGGAT**
CAT RP for construction of MC	CCAGACTCGATCACAGATTTGCCTTCTC
CAT FP for construction of CM[d]	GAGATATACATATGGCTGACAGC
CAT RP for construction of CM	**GGGGAGGCTGTGCTTAAGCTT**CAGATTTGCCTT
MnSOD FP for construction of CM	**AAGCACAGCCTCCCC**
MnSOD RP for construction of CM	TTTCTTTACCCAGACTTATTACTTTTTGCAAGC

[a] FP: forward primer.
[b] MC: MnSOD-CAT fusion gene.
[c] RP: reverse primer.
[d] CM: CAT-MnSOD fusion gene.

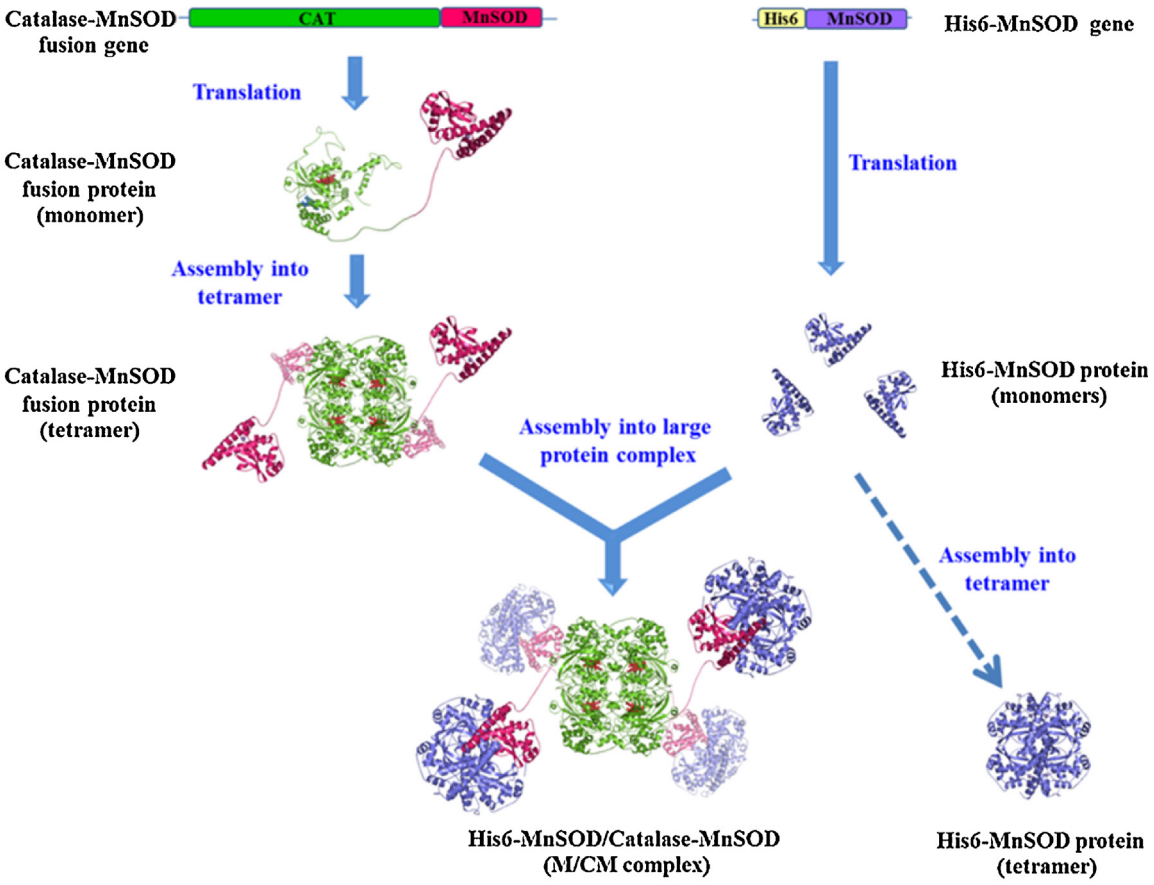

Fig. 1. Schematic representation of the strategy to engineer a bi-functional protein with MnSOD and catalase activities. Co-expression of CAT-MnSOD fusion gene and 6His-MnSOD gene results in monomer of CAT-MnSOD protein and 6His-MnSOD monomer. Then, the two monomers assemble into large multimers of M/CM protein and tetrameric 6His-MnSOD. To produce a tri-functional protein with MnSOD, catalase and cell-permeable activities, 6His-MnSOD gene was replaced by 6His-MnSOD-TAT fusion gene.

2.6. SOD activity assay

The SOD activity assay was slightly modified from that described by Ewing and Janero [16]. The assay was conducted in 1.0 ml total volume consisted of 50 mM phosphate buffer pH 7.4, 50 μM NBT, 33 μM PMS and 78 μM NADH (final concentration). For the assay, 100 μl of sample or standard SOD at various concentrations were pipetted into cuvettes containing 800 μl of reactions mixtures. The reactions were initiated with the addition of 100 μl of 33 μM PMS in 50 mM phosphate buffer pH 7.4. After 5 min incubation at 25 °C, absorbances at 560 nm were measured as an index of NBT reduction. Amount of enzyme (μg) was plotted against % inhibition then SOD activity was calculated for each protein. One unit of SOD activity is defined as the amount of enzyme that causes 50% decrease in NBT reduction.

2.7. Catalase activity assay

Catalase activity was monitored spectrophotometrically as described by Aebi [17]. The assay was performed at 25 °C in 50 mM phosphate buffer pH 7.0. The reaction was initiated by addition of 1.0 ml of 30 mM H_2O_2 into 2 ml of reaction mixture containing protein sample. The decrease in absorbance at 240 nm due to decomposition of H_2O_2 was measured afterward. An extinction coefficient of 43.6 M^{-1} cm^{-1} at 240 nm was applied for calculation. One unit of catalase activity is defined as the amount of enzyme

required to convert 1 μmol of H_2O_2 into water and oxygen per min at 25 °C.

2.8. Heme content analysis of chimeric proteins

Spectral properties of native and chimeric catalases were studied using UV–vis spectrophotometer (UV-1601 SHIMADZU). Protein samples were adjusted to 0.5 mg/ml in sonication buffer, absorbance values ranging from 250 to 700 nm were then measured. The absorbances were plotted against wavelength and R_z ratio (A_{206}/A_{280}) were calculated.

2.9. Investigation of protein internalization into mammalian cells by confocal microscopy

Each purified protein was conjugated with Alexa Fluor® 488 dye according to manufacturer's protocol (Invitrogen, USA). L929 cells were seeded at a density of 10^4 cells per well of four-well chamber slide (Thermo Fisher Scientific Inc., Canada) and incubated for 24 h at 37 °C, 5% CO_2/95% air in humidified condition. Then, the Alexa Flour® 488 conjugated-protein at a final concentration of 0.1 μM was added into culture medium and subjected to 1 h of incubation. Hoechst 33342 was used to stain the nuclei of the cells. After washing with PBS (pH 7.4) 3 times, the cells were fixed with 4% paraformaldehyde for 20 min and the slides were mounted. Internalization of the constructed proteins into L929 cells was followed by Olympus Fluoview FV1000 confocal microscopy and analyzed by Fluoview 3 software.

2.10. Protection of L929 cells against paraquat-induced oxidative stress by chimeric proteins

Protection of L929 cells against paraquat-induced oxidative stress by the fusion proteins was monitored by MTS assay kit according to manufacturer's protocol. Briefly, cells were seeded into 96-well culture plate (Costar, NY, USA) at a density of 10^4 cells per well. After 24 h of incubation, the cells were pre-incubated with MnSOD-TAT or MnSOD-TAT/CAT-MnSOD at 0.00001, 0.0001, 0.001, 0.01, 0.1, 0.2, 1 and 5 SOD units (final concentration in the culture medium) for 1 h. The cells were also pre-treated with CAT-TAT at the same catalase unit found in MnSOD-TAT/CAT-MnSOD. Then, cells were washed for three times with PBS (pH 7.4) and treated with 30 mM paraquat for 5 h. Control experiment was done without addition of protein and paraquat. After oxidative stressor treatment, cells were washed with PBS then 100 μl of DMEM/High glucose supplemented with 10% FBS and 1% gentamycin was added into the culture. Cells were then incubated with 20 μl of MTS reagent for 3 h at 37 °C in the dark. Absorbance values at 490 nm were monitored using Tecan's Infinite M200 PRO microplate reader (Tecan Group Ltd., Switzerland). All measurements were carried out in triplicate. The percentage of cell viability related to control cells was calculated using following formula: % cell viability = $[A_{490nm}$ (test)/A_{490nm} (control)] × 100.

2.11. Statistical analysis

All data are presented as the mean ± standard deviation (SD). All results were analyzed for normal distribution using Kolmogorov–Smirnov test. The null hypothesis was rejected when a probability <0.05. When no significant difference from normality was found, comparison of two means was performed by paired *t*-test. *p*-value < 0.05 with 2-tailed *t*-test was considered statistically significant. All statistical calculations were performed using PASW statistic 18 (SPSS Inc., USA).

2.12. Molecular modeling

The crystal structure of tetrameric human catalase and manganese superoxide dismutase were retrieved from the protein data bank (pdb codes 1DGF and 1N0J, respectively). A single chain model of human CAT fused with MnSOD was constructed on MODELER program v9.12 [18] using those two crystal structures as the templates. The atomic coordinates of the linker region i.e., the C-terminus of CAT (A502–L527) and N-terminus of MnSOD (K1–A15) were then refined on ModLoop web server [19]. The tetrameric structure of the CAT-MnSOD fusion protein was subsequently constructed according to that observed from the human CAT (pdb code 1DGF).

3. Results and discussion

3.1. Production and IMAC purification of chimeric proteins

pETDuet-MC and pETDuet-CM encoding 6His-MnSOD-CAT and 6His-CAT-MnSOD, respectively, were successfully constructed. However, production of both chimeric proteins was not success. Although the chimeras can be expressed as 80 kDa proteins as observed in crude extract by SDS-PAGE analysis, no soluble and active protein was obtained after IMAC purification, suggesting the formation of inclusion bodies. These findings were probably due to the fact that direct genetic fusion resulted in connection of only catalase monomer to SOD monomer, which does not facilitate the formation of their tetrameric structures. Apart from protein band at 80 kDa, expression of 6His-MnSOD-CAT showed degrading protein bands at ~27 kDa (data not shown), suggesting protein instability and fragmentation. In addition, we have modeled a single chain structure of CAT-MnSOD fusion protein using the available structure of human CAT (pdb code 1DGF, [20]) and MnSOD (pdb code 1N0J, [21]) as the templates. The linker region connecting the two enzymes is composed of the last twenty-six C-terminal residues of CAT and the first fifteen N-terminal residues of MnSOD (Fig. 2A). When constructing a tetrameric model of the fusion protein, the forty-one amino acid residues of the linker could give the center-of-mass distance of ~120 Å between CAT and MnSOD structures of the same chain and the distance of ~180 Å between each of the neighboring tetrameric MnSOD (Fig. 2B). Such long distances may be required for the large molecular assemblies without steric hindrance among either inter- or intrachain molecules. In contrast, no extended conformation was observed at the C-terminal region of MnSOD and the N-terminal portion of CAT structures, and thus it suggested the shorter linker region between two enzymes of the MnSOD-CAT fusion protein. Such inappropriate linkage could result in steric hindrance which does not allow the formation of the tetrameric structure of MnSOD-CAT (data not shown). Therefore, based on these findings, only CAT-MnSOD fusion protein was chosen for further study. To enable production of this chimeric protein, the co-expression strategy was applied (Fig. 1). pETDuet-M/CM which allows co-expression of native MnSOD and chimeric CAT-MnSOD (CM) was engineered. The resulting proteins, 6His-MnSOD and chimeric CM were successfully expressed and found to associate into multimeric protein complex (M/CM complex). SDS-PAGE analysis of IMAC purified protein revealed two protein bands at approximately 24 and 80 kDa which corresponded to 6His-MnSOD and chimeric CM, respectively (Fig. 3, lane 8). Since the native MnSOD was designed to contain hexa-histidine tag whereas the chimeric CM was created without purification tag, co-purification of two proteins indicated that the chimeric CM associated with 6His-MnSOD to form a larger protein complex.

To add mammalian cell transduction property to the chimera, HIV-1 TAT transduction domain (TAT) was employed. pETDuet-M-

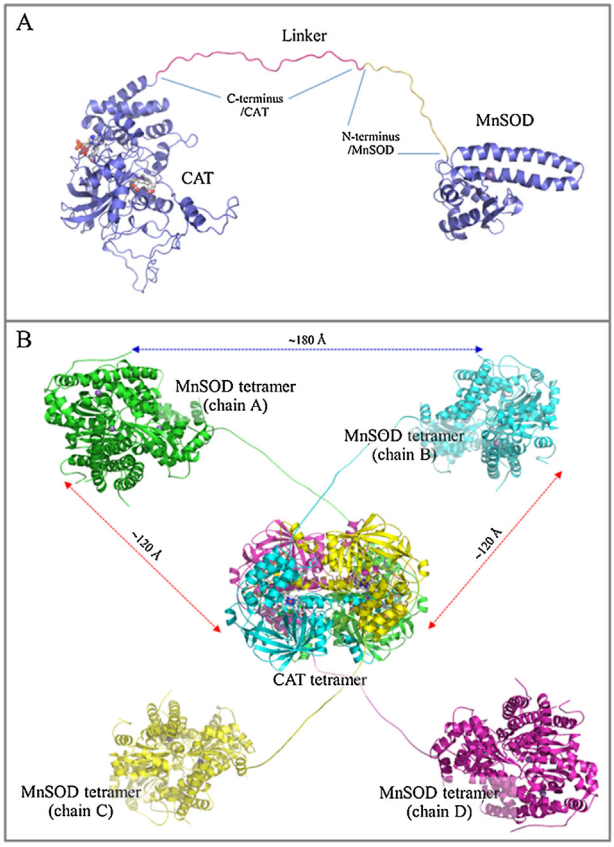

Fig. 2. Structural model of the CAT-MnSOD fusion protein. (A) A model for the single chain of CAT-MnSOD. The linker includes the last twenty-six C-terminal residues 502–527 of CAT and the first fifteen N-terminal residues of MnSOD. (B) A model for the tetrameric CAT-MnSOD. The tetrameric model was constructed according to the crystal structure of tetrameric human CAT (pdb code 1DGF, [3]). The center-of-mass distances between MnSOD and CAT as well as between each neighboring MnSOD are indicated. Heteroatoms including heme, NAD, and Mn^{3+} ions are shown in ball and stick model.

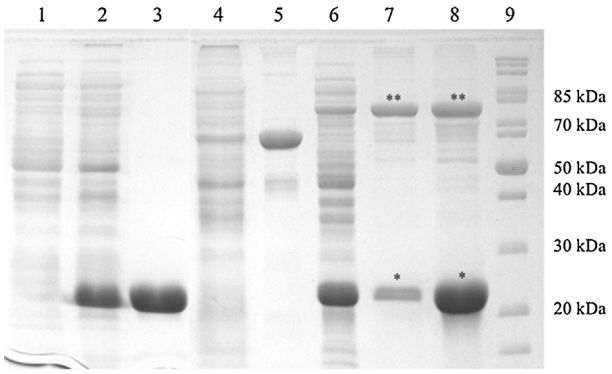

Fig. 3. Expression and purification of native and chimeric proteins. Purified proteins were determined by 12% SDS-PAGE analysis. Lane 1; crude extract of *E. coli* carrying blank pETDuet-1 plasmid, lane 2; crude extract of *E. coli* carrying pET46-MnSOD, lane 3; purified 6His-MnSOD, lane 4; crude extract of *E. coli* carrying pET46-CAT, lane 5; purified 6His-CAT, lane 6; crude extract of *E. coli* carrying pETDuet-MnSOD/CAT-MnSOD, lane 7; purified M/CM complex by gel filtration chromatography, lane 8; IMAC-purified protein from co-expression of 6His-MnSOD and CM, lane 9; protein molecular weight marker (* represents 6His-MnSOD and ** represents CM fusion protein).

TAT/CM which allows co-expression of MnSOD-TAT and chimeric CM was constructed. The expression strategy was the same that shown in Fig. 1 but His6-MnSOD-TAT was used instead of His6-MnSOD. The resulting proteins, 6His-MnSOD-TAT and chimeric

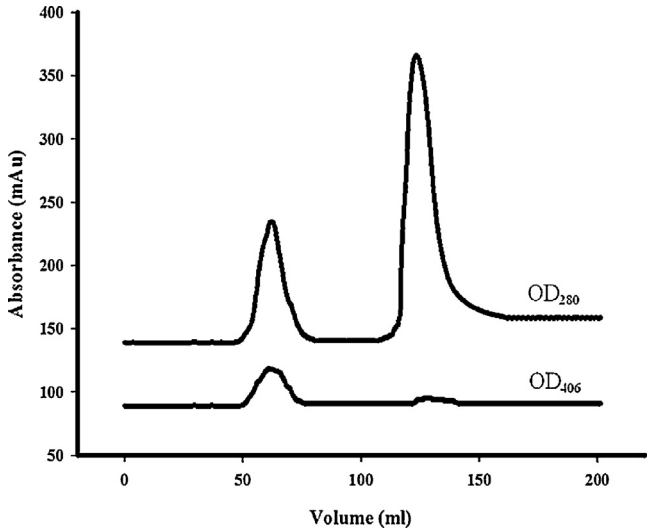

Fig. 4. Chromatogram of gel filtration chromatography performed by Sephacryl S-300HR gel filtration chromatography column. The separated peaks of 6His-MnSOD and M/CM complex were observed by following absorbance at 280 nm and the presence of heme prosthetic group was followed using absorbance at 406 nm.

CM were successfully expressed and purified to homogeneity. SDS-PAGE analysis of the IMAC purified protein revealed two protein bands with molecular weights (MW) resembling to the co-expressed proteins (data not shown). This result indicated that 6His-MnSOD-TAT and chimeric CM also associated into a larger complex as M/CM complex.

3.2. Protein purification and molecular weight determination by gel filtration chromatography

Based on the strategy shown in Fig. 1, the co-expression resulted in two protein complexes, M/CM and tetrameric MnSOD. Both protein complexes possessed hexa-histidine tag, thus they can be co-purified via IMAC. To separate these two complexes, gel filtration chromatography was further applied. The M/CM complex and tetrameric MnSOD were well separated as shown in chromatogram (Fig. 4, OD_{280}). The MW of proteins presented in the first and second peaks were determined to be 630 kDa and 93 kDa which corresponded with the natural MW of M/CM complex and tetrameric MnSOD, respectively (Table 2). In addition, absorbance at 406 nm which represents absorption of typical heme prostatic group of catalase was also measured (Fig. 4, OD_{406}). Only the first peak showed absorption at this wavelength suggesting the presence of catalase in this protein population. SDS-PAGE analysis of protein from the first peak showed two protein bands which corresponded to MnSOD and chimeric CAT-MnSOD (Fig. 3, lane 7). Comparing between IMAC and gel filtration chromatography purified proteins (Fig. 3, lane 7 and 8), the 22 kDa band which corresponding to MnSOD was lighter after gel filtration chromatography. This is probably due to the separation of tetrameric MnSOD from M/CM complex. The MW of the chimera obtained from static light scattering was also consistent with MW from gel filtration chromatography (data not shown). These results together with the heme absorption (Fig. 4, OD_{406}) and the MW determination by both gel filtration chromatography and static light scattering confirmed that the fusion proteins form the complex structure as proposed in Fig. 1.

Additionally, the production of M-TAT/CM gave similar results on gel filtration chromatography as that of the M/CM complex (data not shown). All of the purified fractions were collected and pooled. The purity of the proteins was estimated to be more than

Table 2
Comparison of molecular weights determined by gel filtration chromatography and molecular weights derived from theoretical calculation.

Proteins	Molecular weights by gel filtration chromatography (kDa)	Molecular weights by theoretical calculation (kDa)
6His-MnSOD	93	96
6His-MnSOD-TAT	104	102
6His-CAT-TAT	250	253
6His-MnSOD/Catalase-MnSOD (M/CM)	631	630
6His-MnSOD-TAT/Catalase-MnSOD (M- TAT/CM)	651	649

Table 3
Specific and relative SOD activities of protein samples.

Proteins	Specific SOD activity		Relative SOD activity (%)	
	Units/mg	Units/μmol	Units/mg	Units/μmol
6His-MnSOD	2,270	217,920	100	100
6His-MnSOD-TAT	1,130	107,520	50	54
6His-MnSOD/Catalase-MnSOD (M/CM)	207	137,450	9	63
6His-MnSOD-TAT/Catalase-MnSOD (M- TAT/CM)	168	116,535	7.5	53

Table 4
Specific and relative catalase activities of protein samples.

Proteins	Specific CAT activity		Relative CAT activity (%)	
	Units/mg	Units/μmol	Units/mg	Units/μmol
6His-CAT	13,180	3,241,225	100	100
6His-CAT-TAT	10,810	2,735,360	82	84.5
6His-MnSOD/Catalase-MnSOD (M/CM)	4,315	2,865,450	71	88.5
6His-MnSOD-TAT/Catalase-MnSOD (M- TAT/CM)	4,307	2,952,300	87.5	91

95% homogeneity according to SDS-PAGE analysis. The yields of 6His-CAT, 6His-MnSOD, M/CM, 6His-CAT-TAT, 6His-MnSOD-TAT and M-TAT/CM production were 51, 68, 67, 12, 50 and 14 mg/liter of culture, respectively. The decrease in protein yields after fusion with TAT peptide was evidenced. Though this phenomenon was correlated with our previous studies [13,14], the reason behind was not identified. To avoid this problem, effective CPP with lesser tendency to disrupt the structure and function of the target proteins may be employed [22].

3.3. SOD and catalase activities of chimeric proteins

SOD activity measurement demonstrated that the 6His-MnSOD-TAT, M/CM and M-TAT/CM complexes retained SOD activity up to 54, 63 and 53% as compared to 6His-MnSOD, respectively (Table 3). For catalase activity, 6His-CAT-TAT, M/CM and M-TAT/CM complexes had relative catalase activity up to 84.5, 88.5 and 91%, respectively (Table 4). Although, the engineered proteins had some decrease in SOD and catalase activities (U/μmol), the proteins retained more than 50% enzymatic activities as compared to that of native enzymes. Notably, catalase activities of the M/CM and M-TAT/CM complexes were not significantly different, while SOD activity of the M-TAT/CM complex was slightly decreased comparing to that of M/CM complex. This was probably due to the disturbance at C-terminus by TAT peptide, since this terminus appeared to be important for MnSOD specific activity [21,23].

3.4. Heme content analysis of chimeric proteins

The UV–vis spectrophotometric analysis of the purified proteins showed two absorption maxima at 280 nm and 406 nm which represented total protein and heme prosthetic group of catalase, respectively (Fig. 5). Normally, human catalase has R_z ratio (A_{406nm}/A_{280nm}) about 1.0. According to Fig. 5, the R_z ratio of the 6His-CAT, 6His-CAT-TAT, M/CM and M-TAT/CM were 1.0, 0.99, 0.65 and 0.50, respectively. These results confirmed that the M/CM and M-TAT/CM contained catalase molecule with heme prosthetic group. These results further assured the assembly of either 6His-MnSOD or 6His-MnSOD-TAT with CM as designed in Fig. 1.

3.5. Internalization of chimeric protein into mammalian cells

The fusion proteins were efficiently internalized into L929 fibroblast cells. Treatments were done with 0.1 μM of fluorescent-conjugated 6His-MnSOD, 6His-CAT, 6His-MnSOD-TAT, 6His-CAT-TAT, M/CM and M-TAT/CM for 1 h. No Alexa Flour® 488 fluorescent signal was observed by confocal microscopy in the control cells and cells treated with 6His-MnSOD, 6His-CAT and M/CM (data not shown). However, strong fluorescent signals were detected in 6His-MnSOD-TAT, 6His-CAT-TAT and M-TAT/CM treated cells. Image analysis showed protein localization in both cytoplasm and nucleus of the cells (Fig. 6). These results clearly indicated that the TAT conjugation conferred efficient transduction of the constructed chimeric proteins into mammalian cells. Although all engineered proteins can enter the cells, differences in distribution pattern and fluorescent intensity were observed. 6His-MnSOD-TAT showed the strongest fluorescent intensity among tested proteins and the protein seemed to localize mainly in the cytoplasm of the cells. 6His-CAT-TAT displayed a slight decrease in fluorescent intensity with disperse pattern. M-TAT/CM exhibited moderated fluorescent intensity with clumping pattern of the proteins and mainly localized in the cytoplasmic compartment of the cells.

Our results were in accordance with previous studies that TAT-conjugated peptides localize in both nucleus and cytoplasm of the cells [8,13]. The differences in fluorescent intensity and distribution pattern observed in our study could be due to the properties of transduced proteins such as polarity and availability of TAT peptide on the protein surface [9]. Since initial ionic interaction between TAT peptide and cell surface is required for protein transduction, the polarity of the cargo proteins might disturb this interaction and hamper the transduction efficiency. The importance of TAT peptide exposure on the surface of cargo protein on transduction efficiency was also demonstrated [24]. It has been shown that cell-internalization was abolished when the TAT peptide was

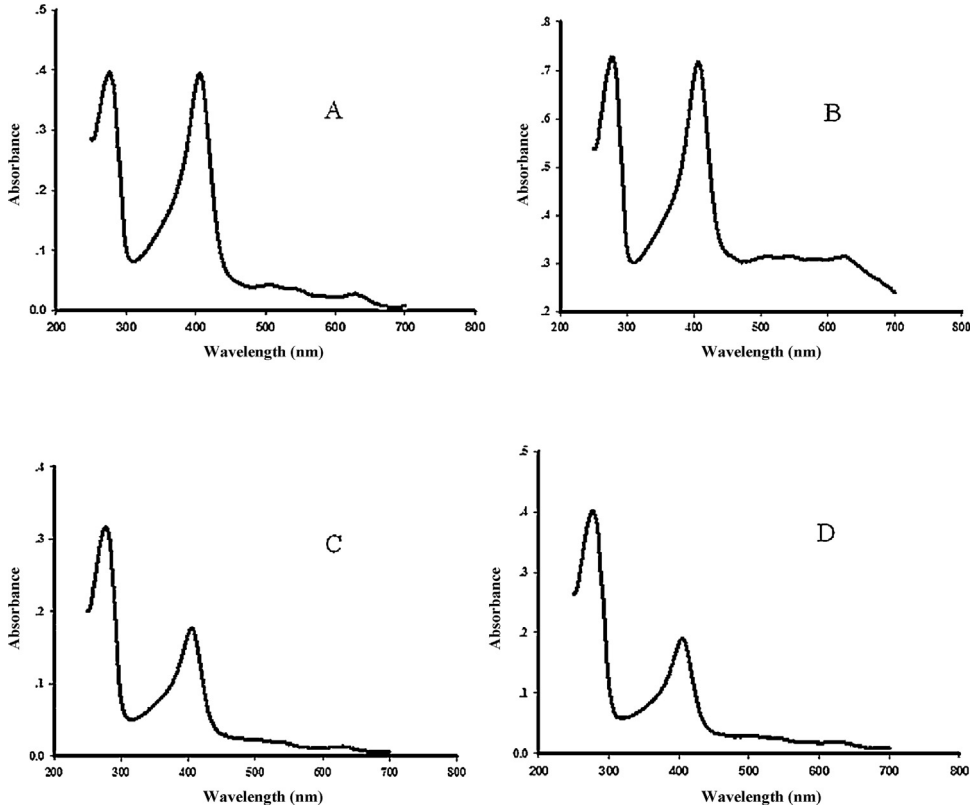

Fig. 5. UV–vis absorption spectra of purified proteins (250–700 nm). The heme absorption peak is represented at 406 nm. (A) 6His-CAT; (B) 6His-CAT-TAT; (C) M/CM and (D) M-TAT/CM.

stericly hindered by cargo surface or by polyethylene glycol coated-surface. In addition, the differences in transduction ability could also depend on the concentration threshold of each protein cargos [25]. Variation in protein cargo concentration was evident for the TAT fusion proteins to equally distribute inside the cells. This was probably due to different properties of the cargos which lead to different transduction efficiency. Another parameter that should be taken into account is the stability of the constructed proteins since it was shown that these transduced proteins can be degraded by both extra- and intracellular proteases and could lead to protein instability and degradation [26]. In addition, efficient transduction of TAT fusion proteins was found to occur in less than 5 minutes of incubation [27]. To investigate the transduction behavior of the M-TAT/CM complex, apart from 1 h, various incubation periods may be applied.

3.6. *Protection of mammalian cells against paraquat-induced oxidative stress*

According to cell internalization ability, only 6His-MnSOD-TAT, 6His-CAT-TAT and M-TAT/CM, which efficiently transduced into L929 cells, were further investigated for their protective effect against paraquat-induced cell death. Paraquat (1,1′-dimethyl-4,4′-bipyridinium dichloride) is a redox cycling agent which rapidly reacts with O_2 to generate intracellular superoxide anions ($O_2^{\bullet -}$). Production of this $O_2^{\bullet -}$ is a primary cause of oxidative stress and cell death [28]. In this study, since the ratio between SOD and catalase activities of M-TAT/CM was found to be 1:25.6 (SOD 168 units/mg protein and catalase 4307 units/mg protein, Tables 3 and 4), SOD and catalase activities in each tested group were adjusted to this ratio. Cultures with addition of only paraquat were considered as 50% viability, and cultures without paraquat and protein treatment were regarded as control with 100% viability.

Pretreatment with both 6His-MnSOD-TAT and M-TAT/CM significantly increased cell viability in each of every tested dose as compared to cells without protein pretreatment (p-value <0.05, Fig. 7). Notably, no significant increase in protection by 6His-MnSOD-TAT was observed when amount of the protein was increased from 0.00001 to 5 SOD units. However, significant increase in protection was observed after pretreatment with 1 and 5 SOD units of M-TAT/CM (p-value < 0.05). The cell viability was brought up to 110% at the maximum M-TAT/CM unit tested. This rising pattern of protection was unique only in the M-TAT/CM but not in other two proteins. Since $O_2^{\bullet -}$ (generated by paraquat treatment) is a substrate of SOD, an increase in protective effect was expected with increasing dose of 6His-MnSOD-TAT. However, in our study, no such increase was observed. This might involve with accumulated H_2O_2 which can potentially disturb cellular redox homeostasis and lead to cell death [7,29,30]. Significant protection by 6His-CAT-TAT was demonstrated at 0.0256 and higher catalase unit comparing to no protein pretreatment group (p-value <0.05). However, notification had to be made that protections at these doses were significantly lower than the protection conferred by 6His-MnSOD-TAT and M-TAT/CM in the same tested doses (p-value <0.05). This poor protective effect of 6His-CAT-TAT could be due to the unmatched substrate used in the study. Further investigation on the chimera's ability to protect against H_2O_2-induced cell death may be performed. In the present study, M-TAT/CM, which conferred SOD and catalase activities, exerted superior protection against oxidative stress than SOD or catalase alone. The superiority was as expected since M-TAT/CM possessed proximity between SOD and catalase active sites which is likely to facilitate the direct transfer of toxic intermediate (H_2O_2) from SOD to catalase. Additionally, protection against paraquat in our study indicated that the protein complex was functionally active for at least 5 h. Different intracellular stabilities of TAT-conjugated proteins were previously

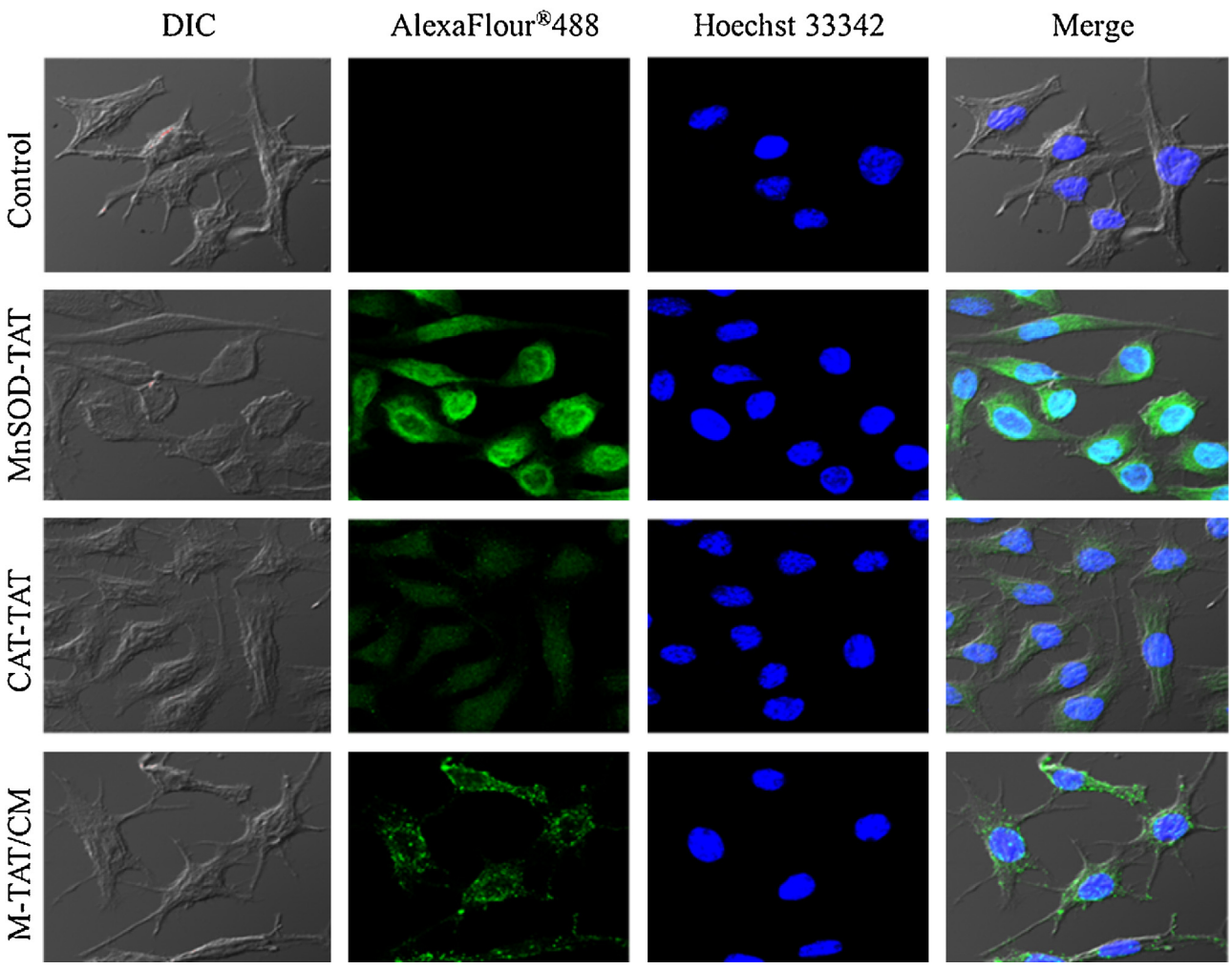

Fig. 6. Transduction of Alexa Flour 488®-labeled 6His-CAT-TAT, 6His-MnSOD-TAT and M-TAT/CM into L929 cells examined by confocal microscopy. Images were captured after L929 cells were treated with 0.1 μM of the target proteins for 1 h. Nuclei of the cells were stained with Hoechst 33342.

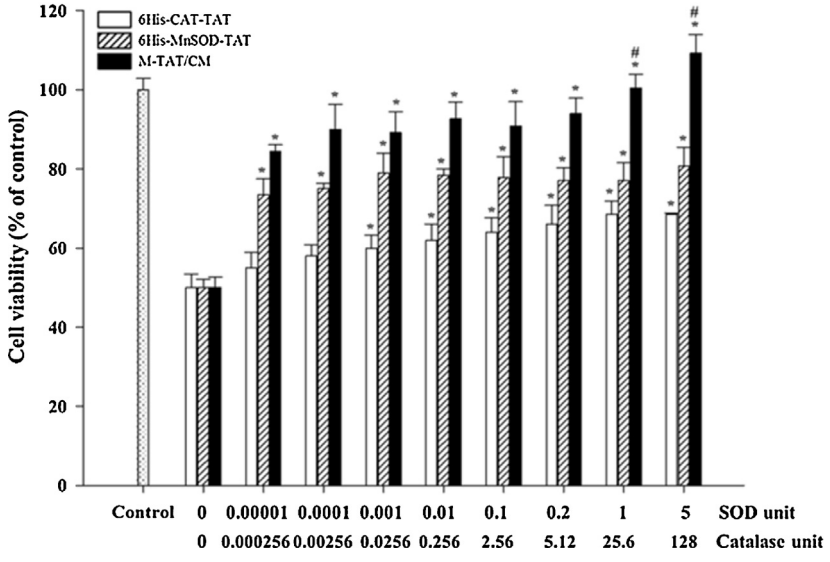

Fig. 7. Protective effect of fusion proteins on paraquat-induced cytotoxicity in L929 cells. Cells were pretreated with varied units of proteins for 1 h. After removal of excess protein, cells were washed and incubated with 30 mM paraquat for 5 h. Cell viability was examined by MTS assay. Data are expressed as mean ± SD from three independent experiments. The statistical analysis was evaluated by paired *t*-test, **p*-value < 0.05 compared to no protein pretreatment group, #*p*-value < 0.05 compared to 6His-CuZnSOD-TAT and 6His-CAT-TAT pretreatment in the same unit.

reported from 24 h to 28 days [9,31]. Thus, our protein complex may be stable for more than 5 h. However, this hypothesis needs to be further investigated.

In conclusion, based on gene and protein engineering, a novel tri-functional protein with MnSOD, catalase and cell-permeable activities has been successfully constructed for the first time. The protein possessed high enzymatic activities and exhibited intracellularly protection against oxidative stress in mammalian cells. This study demonstrated the superiority of using synergistic antioxidant enzymes as protein therapy and protective agents in oxidative stress-related conditions, and presented a novel way that can be applied not only for production of chimeric M/CM and M-TAT/CM but also for production of other chimeras originated as multimeric proteins.

Acknowledgments

This work was supported in part by the Higher Education Research Promotion and National Research University Project of Thailand, Office of the Higher Education Commission. This work was also supported in part by the research grant of Mahidol University (B.E. 2556-2559).

References

[1] M.L. Genova, B. Ventura, G. Giuliano, C. Bovina, G. Formiggini, G.P. Castelli, G. Lenaz, FEBS Lett. 505 (2001) 364–368.
[2] E.M. Gregory, I. Fridovich, J. Bacteriol. 114 (1973) 1193–1197.
[3] S. Damiano, F. Trepiccione, R. Ciarcia, R. Scanni, M. Spagnuolo, L. Manco, et al., Nephrol. Dial. Transplant. 28 (2013) 2066–2072.
[4] B. Parizada, M.M. Werber, A. Nimrod, Free Radic. Res. Commun. 15 (1991) 297–301.
[5] D.W. Kim, D.-S. Kim, M.J. Kim, S.W. Kwon, BMP Rep. (2011) 647–652.
[6] M. Christofidou-Solomidou, A. Scherpereel, R. Wiewrodt, T. Sweitzer, E. Arguiri, Am. J. Physiol. Lung Cell. Mol. Physiol. 285 (2003) 283–292.
[7] G.D. Mao, P.D. Thomas, G.D. Lopaschuk, M.J. Poznansky, J. Biol. Chem. 268 (1993) 416–420.
[8] A. Valdivia, Y. Pérez, R. Cao, M. Baños, A. García1, R. Villalonga, Macromol. Biosci. 7 (2007) 70–75.
[9] H.Y. Kwon, W.S. Eum, H.W. Jang, J.H. Kang, J. Ryu, B.R. Lee, L.H. Jin, J. Park, S.Y. Choi, FEBS Lett. 485 (2000) 163–167.
[10] L. Park, D. Min, H. Kim, J. Park, S. Choi, Y. Park, Diabetes Metab. Res. Rev. 27 (2011) 802–808.
[11] J.S. Wadia, S.F. Dowdy, Curr. Opin. Biotechnol. 13 (2002) 52–56.
[12] R.W. Noble, Q.H. Gibson, J. Biol. Chem. 245 (1970) 2409–2413.
[13] W. Eiamphungporn, S. Yainoy, V. Prachayasittikul, Int. J. Pept. Res. Ther. 21 (2015) 63–67.
[14] S. Yainoy, P. Houbloyfa, W. Eiamphungporn, C. Isarankura-Na-Ayudhya, V. Prachayasittikul, Int. J. Biol. Macromol. 68 (2014) 60–66.
[15] S. Yainoy, C. Isarankura-Na-Ayudhya, T. Tantimongcolwat, V. Prachayasittikul, Pak. J. Biol. Sci. 10 (2007) 3541–3548.
[16] J.F. Ewing, D.R. Janero, Anal. Biochem. 232 (1995) 243–248.
[17] H. Aebi, Methods Enzymol. 105 (1984) 121–126.
[18] A. Sali, T.L. Blundell, J. Mol. Biol. 234 (1993) 779–815.
[19] A. Fiser, A. Sali, Bioinformatics 19 (2003) 2500–2501.
[20] C.D. Putnam, A.S. Arvai, Y. Bourne, J.A. Tainer, J. Mol. Biol. 296 (2000) 295–309.
[21] G.E. Borgstahl, H.E. Parge, M.J. Hickey, W.F. Beyer Jr., R.A. Hallewell, J.A. Tainer, Cell 71 (1992) 107–118.
[22] V.P. Torchilin, Ann. Rev. Biomed. Eng. 8 (2006) 343–375.
[23] Y. Sheng, A. Durazo, M. Schumacher, E.B. Gralla, D. Cascio, D.E. Cabelli, J.S. Valentine, PLoS One 8 (2013) 624–646.
[24] V.P. Torchilin, R. Rammohan, V. Weissig, T.S. Levchenko, Proc. Natl. Acad. Sci. U. S. A. 98 (2001) 8786–8791.
[25] G. Tunnemann, R.M. Martin, S. Haupt, C. Patsch, F. Edenhofer, M.C. Cardoso, FASEB J. 20 (2006) 1775–1784.
[26] R. Fischer, K. Kohler, M. Fotin-Mleczek, R. Brock, J. Biol. Chem. 279 (2004) 12625–12635.
[27] M. Becker-Hapak, S.S. McAllister, S.F. Dowdy, Methods 24 (2001) 247–256.
[28] T. Fukushima, K. Tanaka, H. Lim, M. Moriyama, Environ. Health Prev. Med. 7 (2002) 89–94.
[29] B.A. Omar, J.M. McCord, Free Radic. Biol. Med. 9 (1990) 473–478.
[30] S. Kawanishi, S. Inoue, K. Yamamoto, Biol. Trace Elem. Res. 21 (1989) 367–372.
[31] L. Cao, J. Si, W. Wang, X. Zhao, X. Yuan, H. Zhu, X. Wu, J. Zhu, G. Shen, Mol. Cells 21 (2006) 104–111.